Supplementary Material

Cartilage-bioinspired, tough and lubricated hydrogel based on nanocomposite enhancement effect

Fen Xiao[a], Pengshuo Zheng[a], Jianxin Tang[a], Xin Huang[a], Wenji Kang[a], Guiyin Zhou[a,b*] , Kehui Sun[b]

a *Hunan key laboratory of biomedical nanometer and device, Hunan University of Technology, Zhuzhou 412007, P. R. China*

b *School of Physics and Electronics, Central South University, Changsha 410083, China*

* Corresponding author

E-mail address: gyzhou@hut.edu.cn

XRD Characterization. The distances between adjacent pores of MSNs-NH_2 and MSNs-NH_2@PSPMA are calculated based on the Bragg equation:

$$2d\sin\theta = n\lambda \quad (1)$$

Where d is the interplanar spacing of MSNs-NH_2 and MSNs-NH_2@PSPMA, and n=1, λ=1.54 Å=0.154 nm.

Compressive mechanical test. The compressive strain (ε), compressive stress (σ), compressive modulus (E), and dissipated energy (U_{hys}) were calculated by equations (2-5), respectively:

$$\varepsilon = \frac{\Delta h}{h_0} \times 100\% \quad (2)$$

$$\sigma = \frac{F}{S_0} \quad (3)$$

$$E = \frac{\sigma}{\varepsilon} = \frac{F\Delta h}{S_0 h_0} = K \quad (4)$$

$$U_{hys} = \int_{\varepsilon=0}^{\varepsilon=\varepsilon_x} (\sigma_{load} - \sigma_{unload}) d\varepsilon \quad (5)$$

where Δh and h_0 are the compressive deformation and initial height of hydrogel during loading, respectively, F is the force, S_0 is the original cross-section area, and K is the slope (10-20%) of the compressive stress-strain curve. ε_x is a preset strain, and σ_{load} and σ_{unload} are the corresponding stress levels during the compressive loading-unloading process, respectively.

Tensile mechanical test. The tensile strain (ε), tensile stress (σ), elastic modulus (E), bulk toughness (ω), and dissipated energy (U_{hys}) were calculated by equations (6-10), respectively:

$$\varepsilon = \frac{\Delta l}{l_0} \times 100\% \quad (6)$$

$$\sigma = \frac{F}{A_0} \quad (7)$$

$$E = \frac{\sigma}{\varepsilon} = \frac{F\Delta l}{A_0 l_0} = K \quad (8)$$

$$\omega = \int_{\varepsilon=0}^{\varepsilon=\varepsilon_b} \sigma_{load}\, d\varepsilon \quad (9)$$

$$U_{hys} = \int_{\varepsilon=0}^{\varepsilon=\varepsilon_x} (\sigma_{load} - \sigma_{unload}) d\varepsilon \tag{10}$$

where Δl and l_0 are the elongation and initial length of hydrogel during loading, respectively, F is the force, A_0 is the original cross-section area, and K is the slope (0-10%) of the tensile stress-strain curve. ε_b and σ_{load} are the breaking strain and stress during the loading process. ε_x is a preset strain, and σ_{load} and σ_{unload} are the corresponding stress levels during the tensile loading-unloading process, respectively.

Tearing energy test. The tearing energy (Γ) was estimated by equations (11)

$$\Gamma = \frac{2F_{ave}}{d} \tag{11}$$

where F_{ave} is the average force of peak values during steady-state tear, and d is the thickness of the samples.

Rheological test. A sinusoidal compressive strain (or force) applied to the hydrogel will produce corresponding compressive stress (or strain), the strain (ε), stress (σ), storage modulus (G'), loss modulus (G") and lass factor (tanδ) can be calculated by equations (12-16), respectively:

$$\varepsilon = \varepsilon_0 \sin \omega t \tag{12}$$

$$\sigma = \sigma_0 \sin(\omega t + \delta) \tag{13}$$

$$\mathrm{G}' = \left(\frac{\sigma_0}{\varepsilon_0}\right) \cos \delta \tag{14}$$

$$\mathrm{G}" = \left(\frac{\sigma_0}{\varepsilon_0}\right) \sin \delta \tag{15}$$

$$\tan \delta = \frac{\sin \delta}{\cos \delta} = \frac{\mathrm{G}"}{\mathrm{G}'} \tag{16}$$

Where ω is the frequency, σ_0 and ε_0 is the amplitude of stress and strain respectively, δ is the phase angle between σ and ε.

Swelling test. The swelling ratio (Q_t) of each period and the final equilibrium swelling ratio (Q_{SR}) were recorded and could be calculated as follow equations (17-18):

$$Q_t = W_t / W_0 \tag{17}$$

$$Q_{SR} = W_e / W_0 \tag{18}$$

where W_e and W_0 correspond to the weight of equilibrium swelling hydrogel and sample hydrogel, respectively, and W_t corresponds to the weight of each period of samples.

Cytotoxicity test. The cell viability was calculated as follow:

$$\text{Cell viability (\%)} = (OD_{experient} - OD_{blank}) \ / \ (OD_{control} - OD_{blank}) \times 100\%$$

Where $OD_{experient}$, $OD_{control}$ and OD_{blank} are the absorbance of the sample, the absorbance of the negative control and the absorbance of the blank group, respectively.

Hemolysis test. The relative hemolysis ratio of sample red blood cells was as follow:

$$\text{Relative hemolysis ratio (\%)} = (OD_t - OD_{nc}) \ / \ (OD_{pc} - OD_{nc}) \times 100\%$$

Where OD_t, OD_{nc} and OD_{pc} are the absorbance of the sample, the absorbance of the negative control and the absorbance of the positive control, respectively.

Impact test.

The magnet group consists of five magnets (mass of 10g, diameter of 20 mm and thickness of 5 mm), and the magnetic intensity of magnet group is 1050 Gs. A magnet group was fixed on the table with a silicone sleeve, and another magnet group was hold in hand, the distance between the magnet groups was ~100 mm. The impact test was carried out by the strong magnetic force between the two magnet groups.

Table S1. Mechanical properties comparison of various hydrogels.

Samples	Compressive strength (MPa)	Friction	Biocompatibility	References
Cartilage	3~18	~0.11	Yes	[1]
This work	**6.63~**	**~0.056**	Yes	**This work**
PAMPS-PDMAA	3.1	0.09	N.A.	[2]
TPCS	8.0	0.05	Yes	[3]
Composite-LP	1.0	0.10	N.A.	[4]
PVA-BA/PEG	2.5	0.04	N.A.	[5]
PVA/PAA-Nano	5.22	0.06	No	[6]
Hy-g-PSPMA	2.8	0.047	N.A.	[7]
J-HPCS-HAp	4.4	0.024	Yes	[8]

Table S2. Mesoporous properties of the nanospheres.

Nanospheres	specific surface area (m^2/g)	pore volume (cm^3/g)	pore size (nm)	interplanar spacing (nm)
MSNs-NH_2	125.85	0.453	7.45	5.66
MSNs-NH_2@PSPMA	21.44	0.081	3.79	4.74

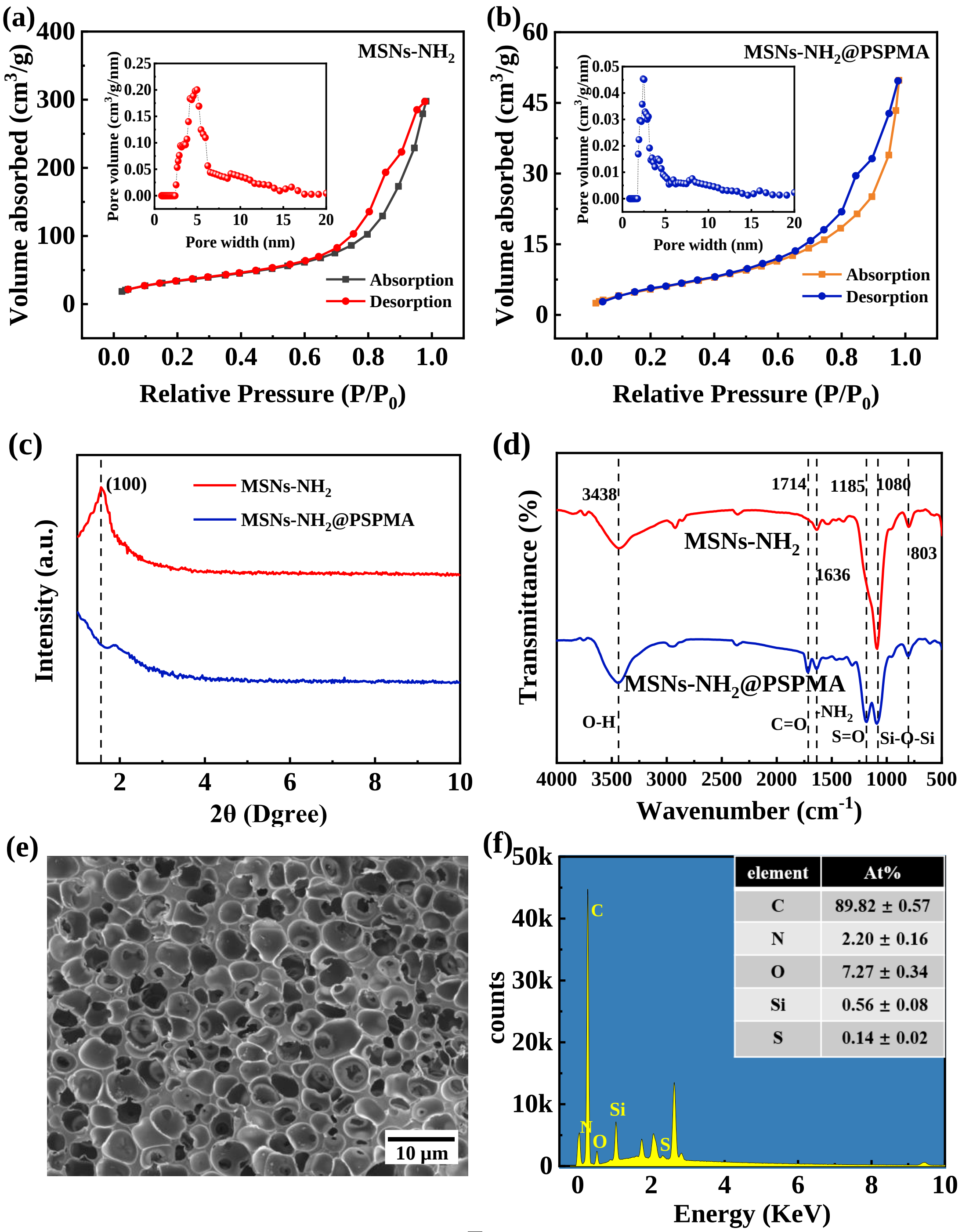

Fig. S1. Nitrogen adsorption-desorption isotherms, and pore size distribution curves (insert) of (a) MSNs-NH_2 and (b) MSNs-NH_2@PSPMA. (c) FTIR spectra, (d) XRD patterns of MSNs-NH_2 and MSNs-NH_2@PSPMA; The (e) SEM images and the element contents (f) of PVA/p(MAAm-co-MAAc) nanocomposite hydrogel. The data are presented as average ± standard deviation and sample size n = 3.

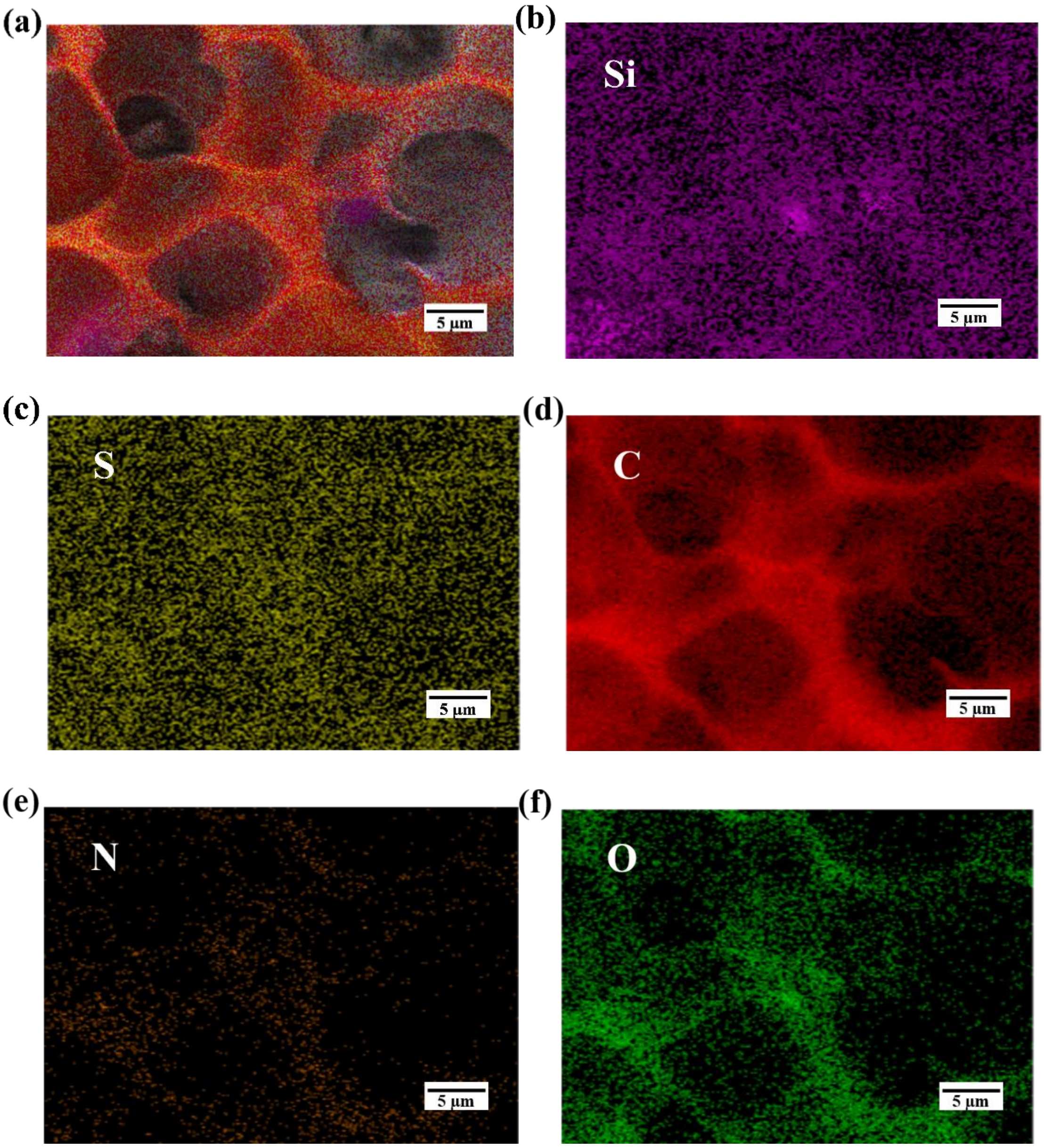

Fig. S2. (a) The layered image images of PVA/p(MAAm-*co*-MAAc) nanocomposite hydrogels from EDS; The electronic image of (b) Si, (c) S, (d) C, (e) N and (f) O.

Table S3 Composition and Mechanical Properties of Hydrogels

Samples	PVA (g)	MAAm (g)	MAAc (g)	MSNs-NH_2@PSPMA (g)	Compressive strength at 50% strain (MPa)	Compressive modulus (MPa)
1	0.40	0.20	1.70	0.000	6.21±0.04	6.81±0.49
2	0.40	0.20	1.70	0.0125	6.32±0.17	7.61±0.37
3	0.40	0.20	1.70	0.0250	6.63±0.11	8.88±0.42
4	0.40	0.20	1.70	0.0375	7.07±0.08	8.31±0.81
5	0.40	0.20	1.70	0.050	8.27±0.28	7.15±0.30

The data are presented as average ± standard deviation and sample size n = 3.

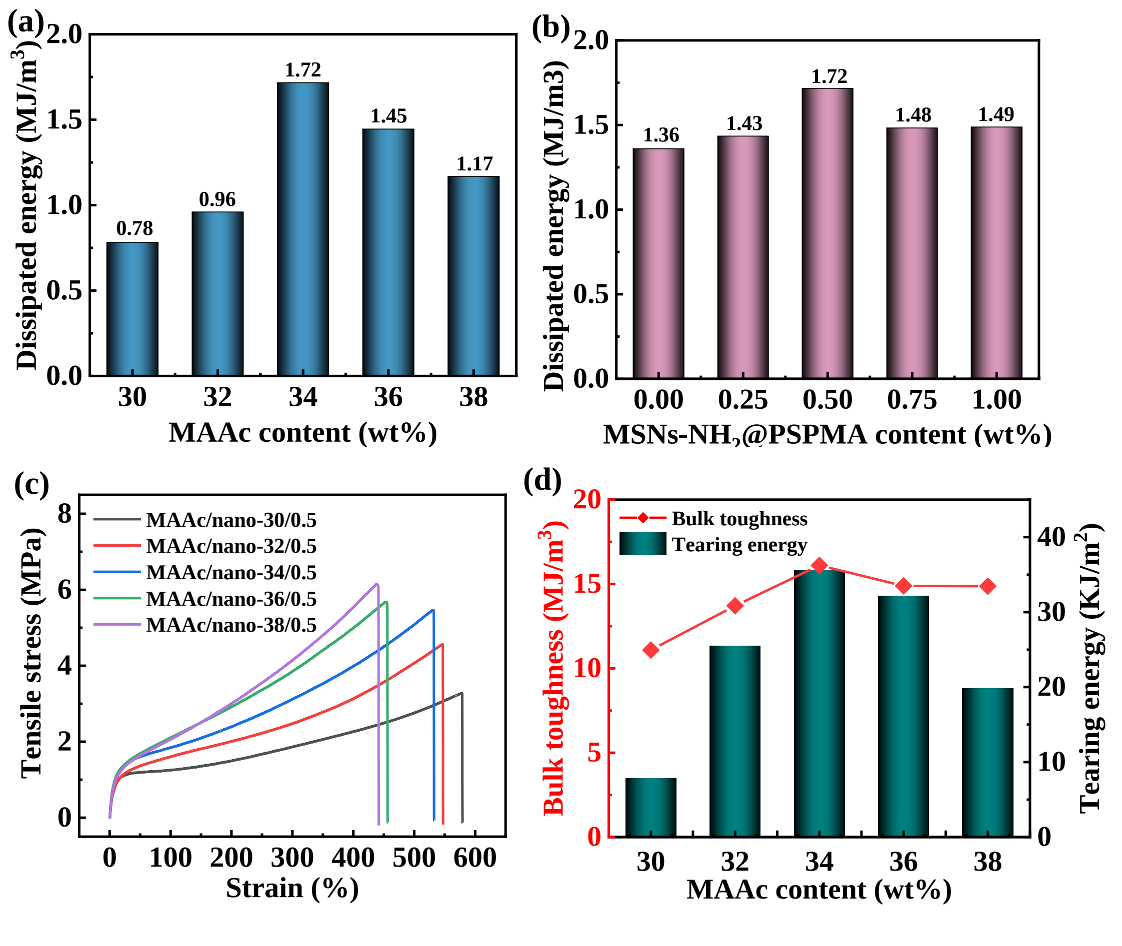

Fig. S3. The dissipated energy of PVA/p(MAAm-*co*-MAAc) nanocomposite hydrogels for different (a) MAAc content and (b) nanospheres content; (c) the tensile strain and tensile strength, (d) the bulk toughness and tearing energy of PVA/p(MAAm-*co*-MAAc) nanocomposite hydrogels.

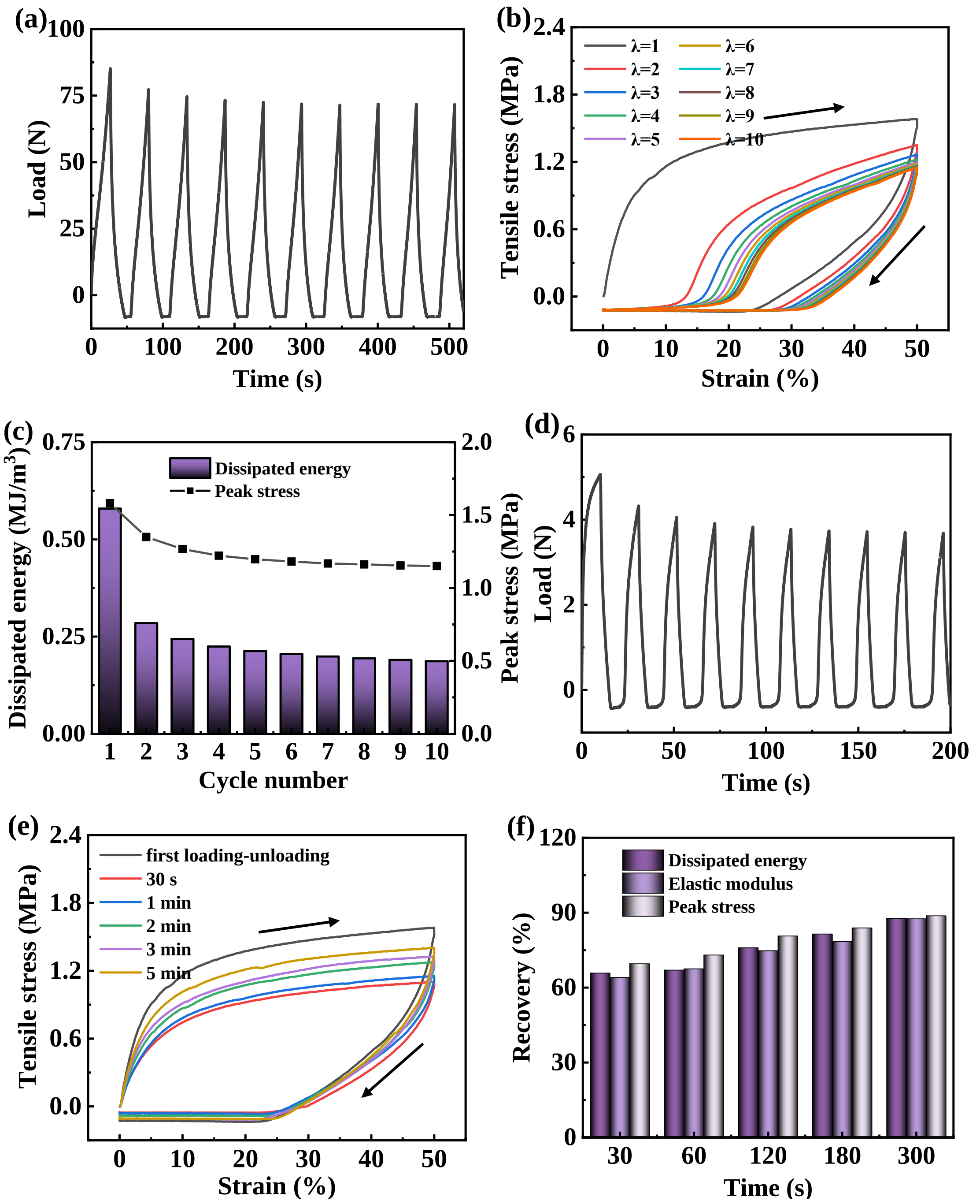

Fig. S4. (a) Load-time curves of PVA/p(MAAm-co-MAAc) nanocomposite hydrogels at the compressive strain of 30% (b) Loading-unloading cyclic tensile stress-strain curves, (c) dissipated energy and peak stress, and (d) load-time curves of PVA/p(MAAm-*co*-MAAc) nanocomposite hydrogels at the strain of 50%; (e) Loading-unloading cyclic tensile stress-strain curves of PVA/p(MAAm-*co*-MAAc) nanocomposite hydrogels at the strain of 50% after resting 30 s, 1 min, 2 min, 3 min, and 5 min, respectively; (f) The recovery of dissipated energy, elastic modulus, and peak stress after resting 30 s, 1 min, 2 min, 3 min, and 5 min, respectively.

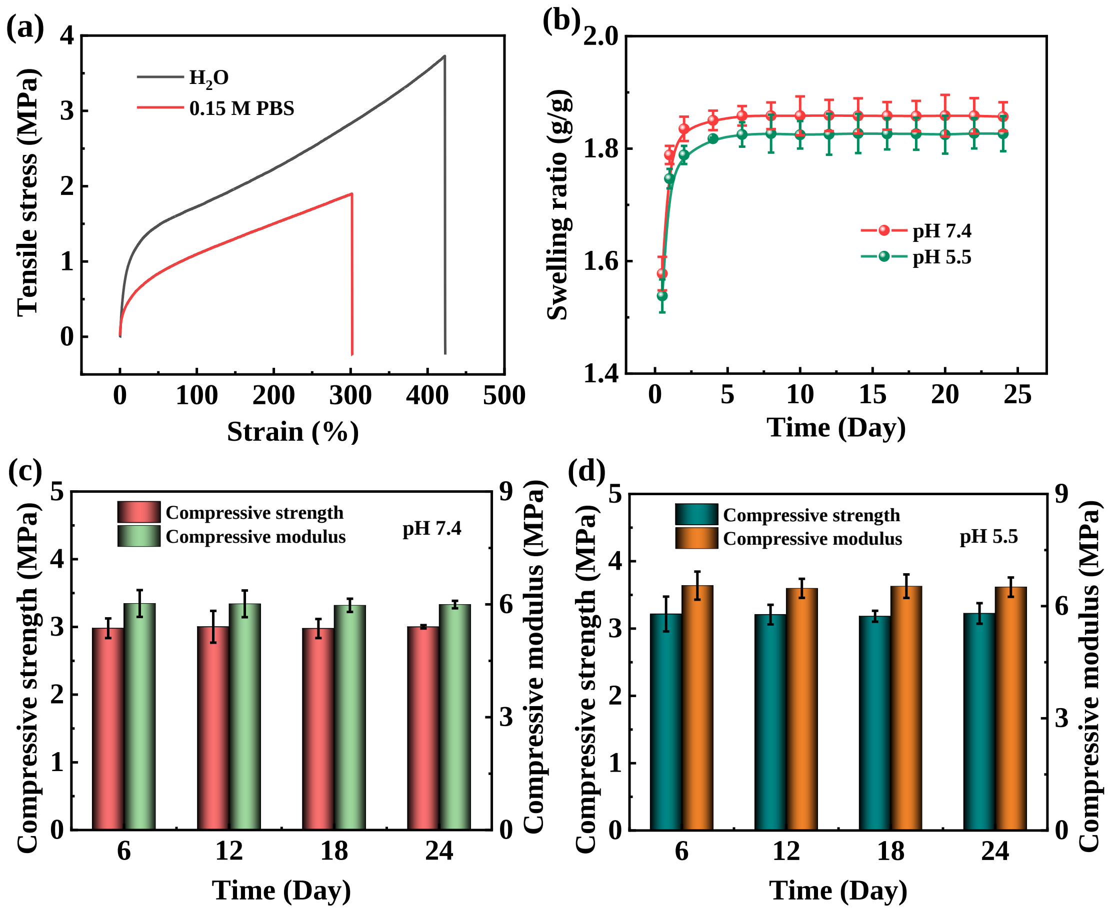

Fig. S5. (a)Tensile stress-strain curves of PVA/p(MAAm-*co*-MAAc) nanocomposite hydrogels after swelling to equilibrium in DI water and 0.15 M PBS buffer solution. (b) Swelling curves of PVA/p(MAAm-*co*-MAAc) nanocomposite hydrogels in pH 7.4 and pH 5.5 of PBS buffer solution at 37°C. (c-d) The compressive strength and compressive modulus of PVA/p(MAAm-*co*-MAAc) nanocomposite hydrogels in pH 7.4 and pH 5.5 of PBS buffer solution at 37°C, respectively. The data are presented as average ± standard deviation and sample size n = 3.

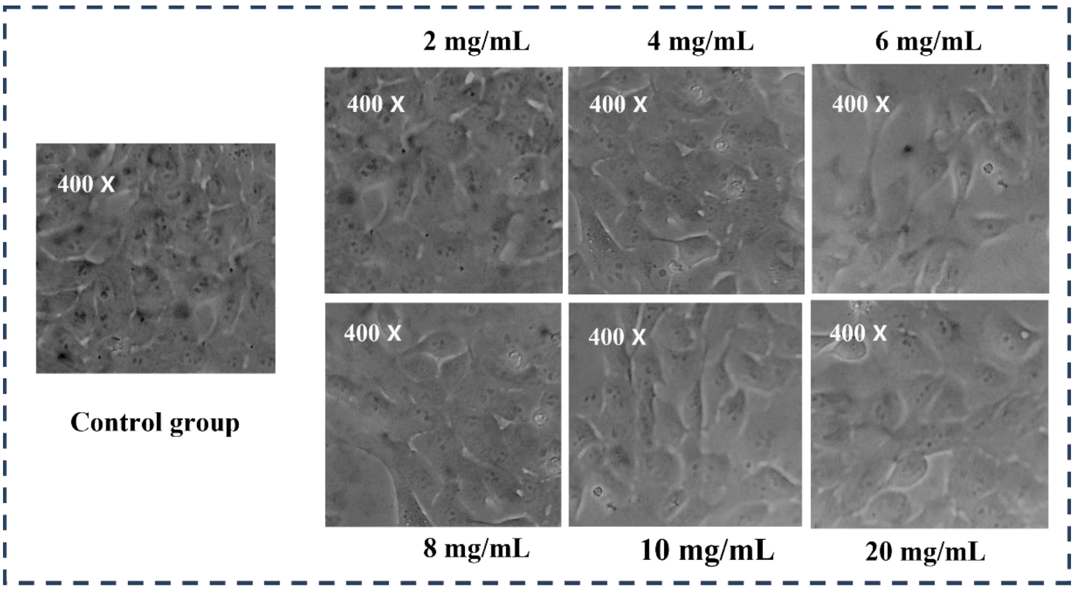

Fig. S6. The optical microscope image of MCF-10A cell co-cultured with the experiment concentrations of the gel solutions.

References

[1] Means AK, Grunlan MA. Modern Strategies To Achieve Tissue-Mimetic, Mechanically Robust Hydrogels. Acs Macro Letters. 2019;8(6):705-13.
[2] Yang F, Zhao J, Koshut WJ, Watt J, Riboh JC, Gall K, et al. A Synthetic Hydrogel Composite with the Mechanical Behavior and Durability of Cartilage. Advanced Functional Materials. 2020;30(36):2003451.
[3] Luo C, Guo A, Zhao Y, Sun X. A high strength, low friction, and biocompatible hydrogel from PVA, chitosan and sodium alginate for articular cartilage. Carbohydr Polym. 2022;286:119268.
[4] Zhao W, Zhang Y, Zhao X, Ji Z, Ma Z, Gao X, et al. Bioinspired Design of a Cartilage-like Lubricated Composite with Mechanical Robustness. ACS Appl Mater Interfaces. 2022;14(7):9899-908.
[5] Cui L, Tong W, Zhou H, Yan C, Chen J, Xiong D. PVA-BA/PEG hydrogel with bilayer structure for biomimetic articular cartilage and investigation of its biotribological and mechanical properties. Journal of Materials Science. 2020;56(5):3935-46.
[6] Chen Q, Zhang X, Chen K, Wu X, Zong T, Feng C, et al. Anisotropic hydrogels with enhanced mechanical and tribological performance by magnetically oriented nanohybrids. Chemical Engineering Journal. 2022;430:133036.
[7] Liu H, Zhao X, Zhang Y, Ma S, Ma Z, Pei X, et al. Cartilage Mimics Adaptive Lubrication. ACS Appl Mater Interfaces. 2020;12(45):51114-21.
[8] Luo C, Guo A, Li J, Tang Z, Luo F. Janus Hydrogel to Mimic the Structure and Property of Articular Cartilage. ACS Appl Mater Interfaces. 2022;14(31):35434-43.